Title

Numerical Modeling of Deformation Response of Embankment Subjected to Rainfall Infiltration Considering the Hydro-Mechanical Coupled Behavior of Unsaturated Soils

Authors

Wu, Hao

McCartney, John S

Zheng, Yewei

Publication Date

2024-02-22

DOI

10.1061/9780784485354.034

Peer reviewed

Numerical Modeling of Deformation Response of Embankment Subjected to Rainfall Infiltration Considering the Hydro-Mechanical Coupled Behavior of Unsaturated Soils

Hao Wu[1], John S. McCartney[2], Ph.D., P.E., F.ASCE, and Yewei Zheng[3], Ph.D., A.M.ASCE

[1] Master Student, School of Civil Engineering, Wuhan University, Wuhan, Hubei, 430072 China; Email: ahwuhao@whu.edu.cn

[2] Professor, Department of Structural Engineering, University of California, San Diego, La Jolla, CA, 92093-0085, USA; Email: mccartney@ucsd.edu

[3] Professor, School of Civil Engineering, Wuhan University, Wuhan, Hubei, 430072 China; Email: yzheng@whu.edu.cn (corresponding author)

ABSTRACT

Embankments constructed using compacted fill are typically initially in an unsaturated condition. Deformations of embankments may occur due to softening effects associated with rainfall infiltration. In this study, a hydro-mechanical coupled constitutive model was implemented in the finite difference program FLAC2D using the Two-Phase Flow option to simulate the hydro-mechanical behavior of unsaturated soil during infiltration. The model adopts Bishop's effective stress, which considers the combined effects of suction and degree of saturation on the stress-strain behavior and the effect of suction on the stiffness and hardening parameters. The implemented constitutive model was first calibrated using experimental data from triaxial tests. Numerical simulations indicate that as water infiltrates into a 6 m-tall embankment with an inclination of 1:1.5, the differential settlement between the centerline and edge of the embankment increases, with a maximum differential settlement of 80 mm after 96 hours of rainfall. The maximum lateral displacement of the embankment slope also increases to 130 mm after 96 hours. A potential failure surface appears to initiate at a shallow depth of approximately 2 m from the slope surface after the embankment approaches saturation.

INTRODUCTION

Although embankments constructed from compacted soils often remain in unsaturated conditions if they have appropriate drainage, rainfall infiltration can cause softening which may lead to deformations under the self-weight of the embankment soil (Le et al. 2003). While many studies have focused on rainfall-induced stability issues, prediction of the wetting-induced deformation response of embankments can be important to

consider in the design. Wetting-induced deformations of embankments can lead to distress of overlying roadways or even slope failure, resulting in significant economic costs for maintenance and repair.

Wetting of unsaturated soils causes changes in the degree of saturation and suction, which could lead to changes in volume and shear strength, and possibly water retention behavior (Zhou et al. 2012). Alonso et al. (1990) proposed an elastoplastic constitutive model for unsaturated soils, referred to as the Barcelona Basic Model (BBM), using the net stress and suction as two independent stress state variables. While other constitutive models for unsaturated soils have been proposed following the framework of the BBM (e.g., Wheeler and Sivakumar 1995), an issue is that hydro-mechanical coupled effects cannot be considered in BBM, which could have crucial effects on the deformation response of unsaturated soils (Zhang and Ikariya 2011). For this reason, several hydro-mechanical coupled constitutive models for unsaturated soils have been proposed in recent decades (Gallipoli et al. 2003; Wheeler et al. 2003; Sun et al. 2007; Xiong et al. 2019; Zhou et al. 2012). For example, Sun et al. (2007) proposed an elastoplastic model for unsaturated soils, which considers the effect of hydraulic behavior on the mechanical behavior using the Bishop's effective stress as the stress state variable, and the effect of void ratio on the soil water retention curve (SWRC) is also considered.

Due to the complex form of these constitutive models for unsaturated soils, few have been implemented into commercial computer programs. One of the most-popular implementations of the BBM is in CODE_BRIGHT (Olivella et al. 1996), which has been applied to a range of engineering problems. Rutqvist et al. (2011) implemented a thermo-elasto-plastic version of BBM into the TOUGH-FLAC simulator to analyze the behavior of unsaturated soils in nuclear waste repositories, which incorporates the suction-induced strains by equivalent mean net stresses. Zheng et al. (2017) investigated the wetting-induced deformations of unsaturated embankments using the BBM implemented in FLAC. However, these numerical simulations involving BBM did not consider the hydro-mechanical coupled behavior of unsaturated soils.

In this paper, a hydro-mechanical coupled constitutive model for unsaturated soil is proposed, which accounts for the effect of degree of saturation on the stress-strain behavior and the effect of void ratio on the water retention behavior. The proposed model is implemented in the two-dimensional finite difference program FLAC and calibrated using experimental data from triaxial tests. The calibrated constitutive model for unsaturated soil is used to simulate the behavior of an unsaturated embankment subjected to rainfall infiltration.

HYDRO-MECHANICAL COUPLED CONSTITUTIVE MODEL

In this study, the Two-Phase Flow option in FLAC is used to implement the constitutive model. In this option, Bishop's effective stress is used to account for the effect of degree of saturation on the stress-strain behavior using the degree of saturation as the effective stress parameter χ. The effect of void ratio on the van Genuchten (1980) soil water retention curve (SWRC) is incorporated using FISH functions in FLAC to account for

the effect of stress-strain behavior on the water retention behavior. The effects of suction on the hardening and stiffness parameters of unsaturated soils are also incorporated using FISH functions.

Stress-Strain Behavior

The mechanical part of the hydro-mechanical model for unsaturated soils is similar to the model proposed by Sun et al. (2007). The mean effective stress p' and the suction s are used as the stress state variables, and the expression is as follows:

$$\sigma' = \sigma - u_a + S_r s \tag{1}$$

where p is the mean total stress, S_r is the degree of saturation, and u_a is the pore-air pressure. The yield surface, f, in the p-q plane is expressed as

$$f = q^2 + M^2 p' \left(p' - p'_y \right) = 0 \tag{2}$$

where

$$p'_y = p'_n \left(p_{0y} / p'_n \right)^{(\lambda(0)-\kappa)/(\lambda(s)-\kappa)} \tag{3}$$

$$\lambda(s) = \lambda(0) + \lambda_s s / \left(p_{at} + s \right) \tag{4}$$

where q = deviatoric stress; p'_y = preconsolidation stress at suction s; M = slope of critical state line; p'_n = mean effective stress with no deformation when suction decreases, which is the stress corresponding to the intersection of compression curves for different suctions; p'_{0y} = preconsolidation stress at saturation; $\lambda(0)$ = slope of normal consolidation line (NCL) for saturated condition; $\lambda(s)$ = slope of NCL at suction s; κ = swelling index; p_{at} = atmospheric pressure; and λ_s = material parameter that controls soil stiffness as a result of changes in suction.

Eq. (3) describes the loading collapse (LC) yield curve in the p-s plane. When the stress state is inside the LC yield curve, the elastic volumetric strain increment $d\varepsilon_v^e$ is calculated as follows:

$$\mathrm{d}\varepsilon_v^e = \kappa \mathrm{d}p' / (1+e) p' \tag{5}$$

where e is the current void ratio. When the stress state is on the LC yield curve, the plastic volumetric strain increment $d\varepsilon_v^p$ is calculated as follows:

$$\mathrm{d}\varepsilon_v^p = (\lambda(0) - \kappa) \mathrm{d}p_{0y} / (1+e) p_{0y} \tag{6}$$

Water Retention Behavior

The SWRC describes the relationship between the degree of saturation S_r and suction s. The van Genuchten (1980) SWRC model is used in FLAC in the following form:

$$S_r = \left(1 / \left[1 + (\alpha s)^n \right] \right)^m \tag{7}$$

where α, m, and n are fitting parameters with m = 1-1/n.

To consider the effect of volume change on the water-retention behavior, the relationship between the void ratio e and the parameter α is incorporated in the van Genuchten model. Nuth and Laloui (2008) proposed a linear relationship between e and $1/\alpha$, as shown in Eq. (8), where A and B are fitting parameters.

$$1/\alpha = -A \times e + B \tag{8}$$

MODEL VERIFICATION

Sun et al. (2007) conducted a series of triaxial tests on compacted clay involving wetting paths. Figure 1 shows the stress and wetting paths (B'C'D'E'F'G'H') of the triaxial tests. In FLAC, single element simulation is conducted under axisymmetric condition to simulate the triaxial tests, and the model parameters are presented in Table 1.

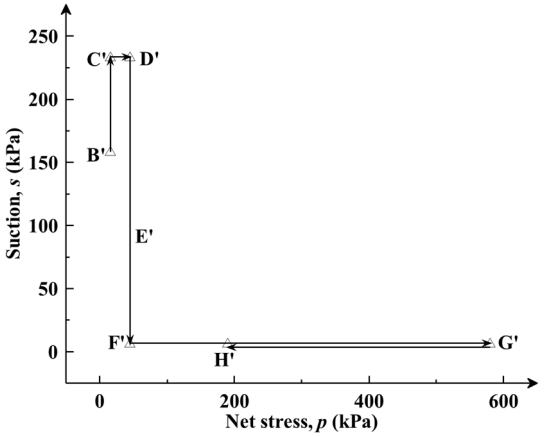

Figure 1. Stress and wetting paths of triaxial tests (from Sun et al. 2007).

Table 1. Model parameters for compaced clay (after Sun et al. 2007).

Mechanical parameter	Value	Hydraulic parameter	Value
Density, ρ_g (kg/m^3)	1700	Water density, ρ_w (kg/m^3)	1000
Compression index, $\lambda(0)$	0.12	Parameter, $1/\alpha$	1322
Swelling index, κ	0.03	Parameter, n	1.136
Critical state parameter, M	1.1	Horizontal permeability coefficient, k_h (cm/s)	10^{-6}
Specific volume, v	2.35		
Atmospheric pressure, p_{at} (kPa)	101	Vertical permeability coefficient, k_v (cm/s)	10^{-7}
Poisson's ratio, v	0.3		
Reference mean effective stress, p'_n (MPa)	1.7		

Figure 2 shows the comparisons between the experimental data and simulation results. The specific volume v decreases with the decrease of suction s in the wetting path D'-E'-F', and the amount of volume change is in good agreement with the experimental data. In general, the simulated results are in reasonable agreement with the experimental data with respect to both mechanical and hydraulic response, which indicates that the proposed model can accurately capture the hydro-mechanical coupled behavior of unsaturated soils subjected to wetting.

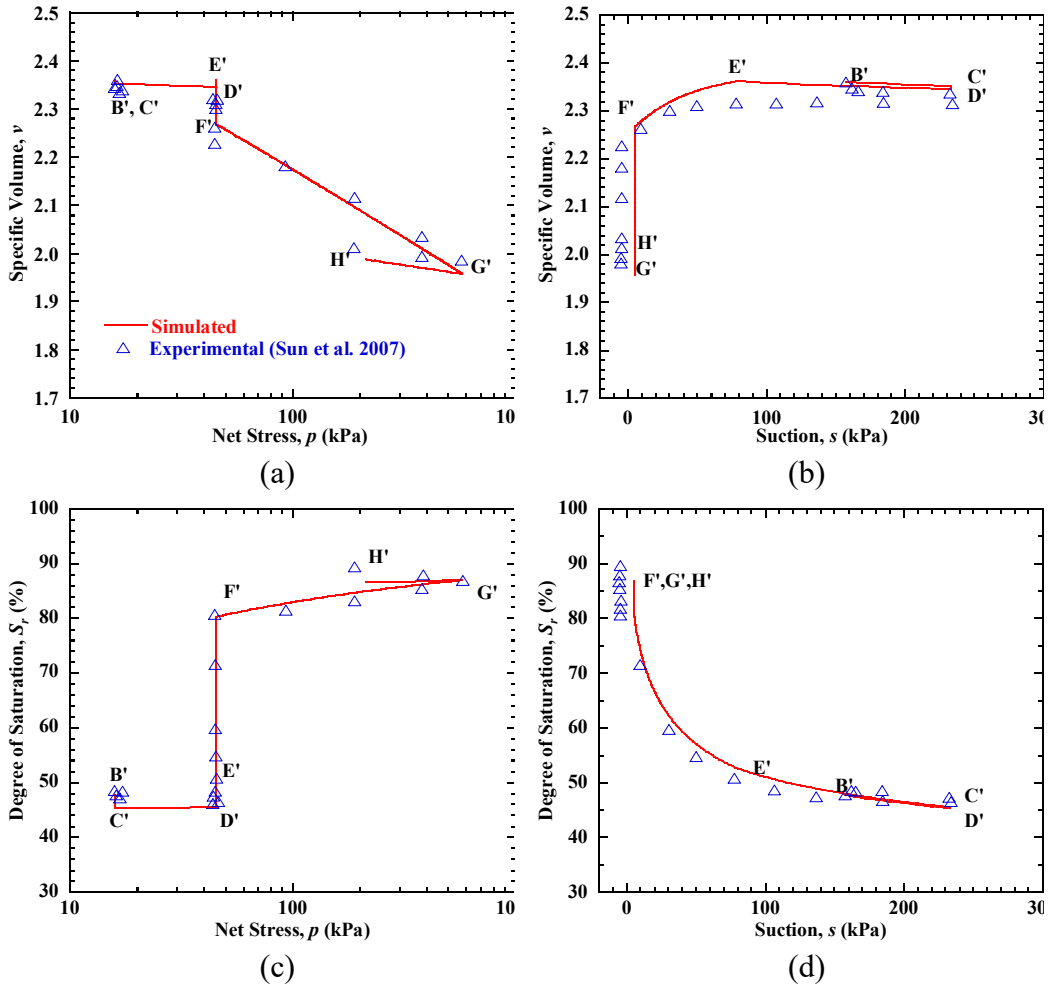

Figure 2. Comparison between experimental and simulated results of triaxial test.

EMBANKMENT SUBJECTED TO RAINFALL INFILTRATION

Embankment Model

The verified hydro-mechanical coupled constitutive model is used to study the wetting-induced deformation behavior of an unsaturated embankment subjected to rainfall infiltration. Since the embankment is a symmetric structure, only half of the embankment is simulated. Figure 3 shows the geometry and boundary conditions of the embankment model. The height of embankment is 6 m, the width of roadway is 8 m, and the side slope ratio is 1:1.5 (horizontal to vertical). The foundation soil has a depth of 6 m and width of 30 m. The bottom boundary of the model was fixed in the vertical and horizontal directions, and the left- and right-side boundaries were fixed in the horizontal direction. The bottom and the left side are set as impermeable boundaries. The top and right side of the model were set as seepage boundaries. The rainfall intensity was set as 10 mm/day to simulate a light rainstorm (Zhao et al. 2020).

The compacted pearl clay used for model verification was selected as the embankment fill and simulated using the verified hydro-mechanical coupled model with calibrated parameters shown in Table 1. A minimum relative compaction of 95% is typically required for the construction of compacted embankment fill. Tatsuoka and Gomes (2018) found that the optimal degree of saturation is around 80%, and S_r ranges from -20% to +5% of the optimum to ensure the relative compaction greater than 95%. Therefore, the initial degree of saturation of 70% was used for the compacted fill. The foundation soil was simulated using the Mohr-Coulomb model, and the water table was assumed to be at the foundation soil surface, thus water infiltration would not affect the behavior of foundation soil. This water table location implies that upward water flow into the embankment will occur due to capillary rise. However, the simulations were started at the end of compaction rather than when the embankment had reached hydraulic equilibrium to represent the conditions expected in a newly-constructed embankment.

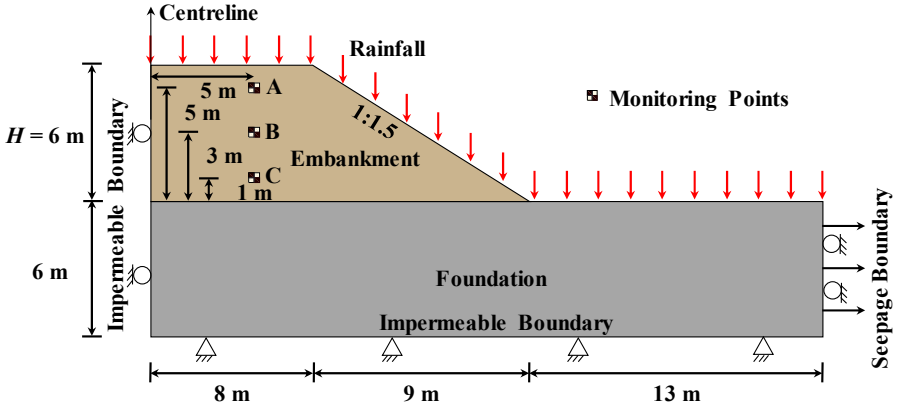

Figure 3. Geometry and boundary conditions of embankment model.

Simulation Results

Simulation results focus on the development of hydro-mechanical response of unsaturated embankment during rainfall infiltration, including saturation and suction distributions, embankment surface settlements, slope lateral displacements, and shear strains within the embankment.

As indicated in Figure 3, three points (i.e., A, B, and C) at 5 m away horizontally from the embankment centerline but at different elevations were monitored during rainfall infiltration. The relationships of suction and saturation versus time is shown in Figure 4(a). When water infiltrates into the unsaturated embankment, the degree of saturation increases, and suction also decreases. The moment of change in degree of saturation is the time of water infiltration reaching the point. The infiltration time is 8 hours at point A, 28 hours at point B, and 59 hours at point C. Figure 5 shows the distribution of degree of saturation at different times during rainfall infiltration. The water infiltrates from the slope surface and the top of embankment into the embankment fill. The surface layer, including embankment top and side slope, becomes saturated at approximately 48 hours. After that, the wetting front moves within the embankment, and

the depth of infiltration is nearly the same from both the embankment top and the side slope. Figure 4(b) shows the change of suction and settlement versus time. The development of settlement lags behind the variation of suction. For example, suction at point A starts to decrease from 12 hours, while the settlement at the same elevation starts to accumulate from 36 hours. As the water infiltrates from the top of embankment, the settlement at higher elevation accumulates rapidly first, and then the settlement at lower elevation develops. In general, the settlement at higher elevation is much larger than those at lower elevation.

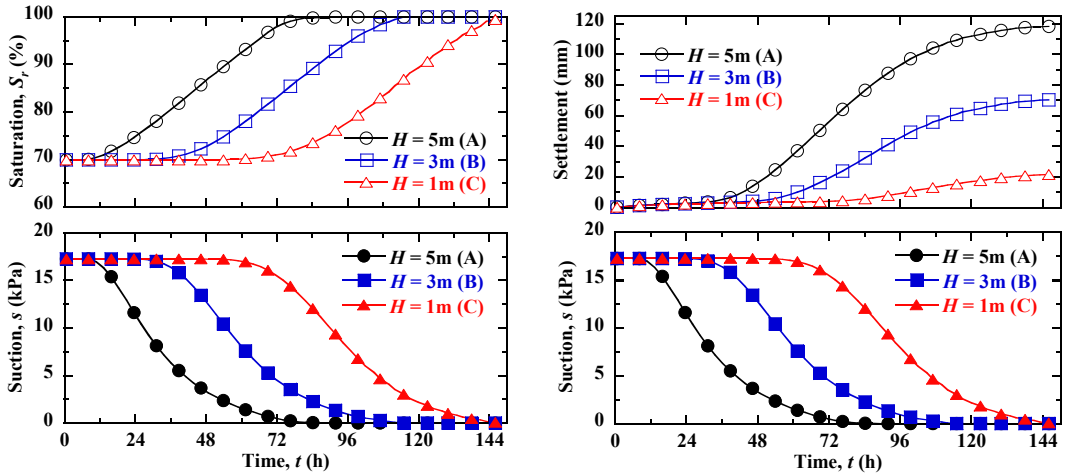

Figure 4. Monitored response during rainfall infiltration: (a) suction and saturation vs. time; (b) suction and settlement vs. time.

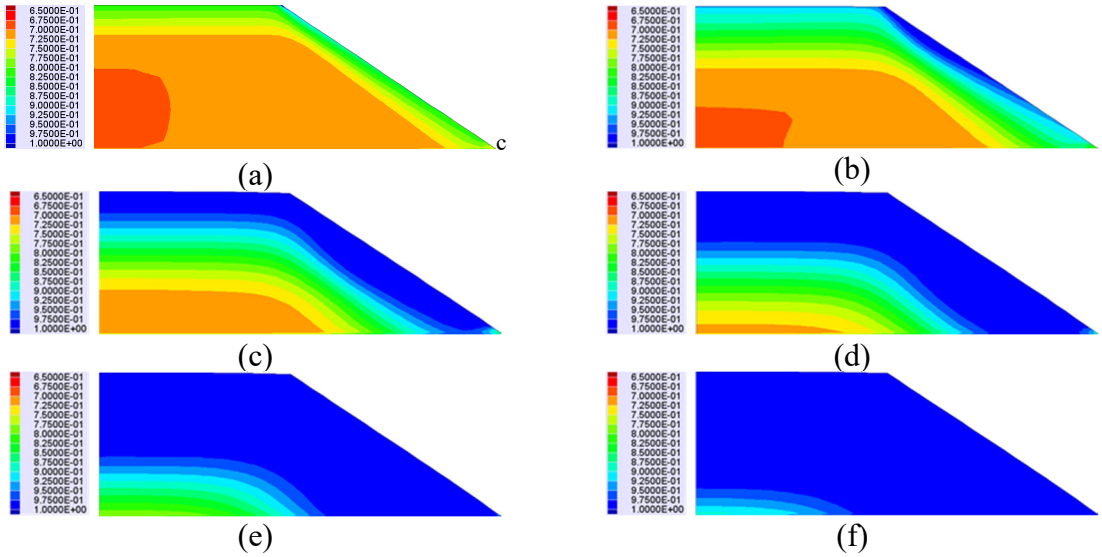

Figure 5. Distributions of degree of saturation: (a) T = 24h; (b) T = 48h; (c) T = 72h; (d) T = 96h; (e) T = 120h; (f) T = 144h.

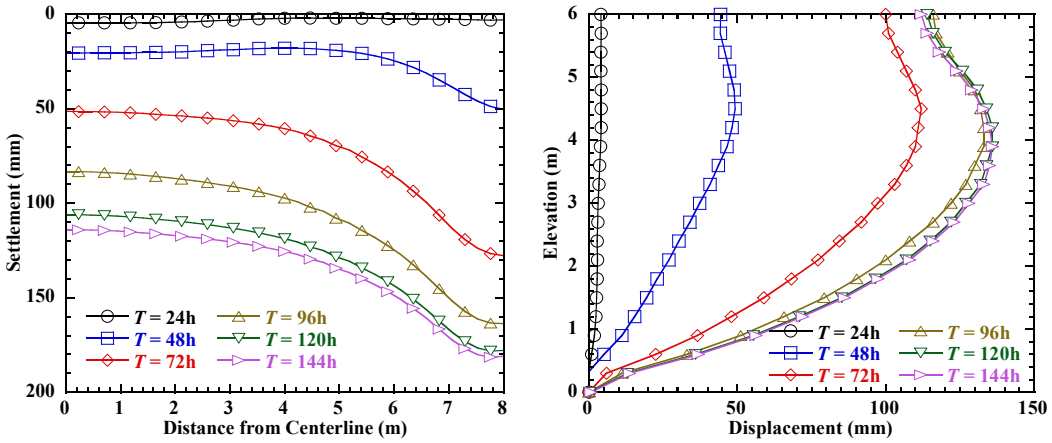

Figure 6. Displacement profiles: (a) embankment top settlement; (b) slope lateral displacement.

Figure 6(a) shows the settlements of the embankment top surface during rainfall infiltration due to the decrease of suction. After 24 hours, the top surface settlement is nearly uniform at 2 mm. The differential settlement between the centerline and side develops after that time. The settlement is 20 mm at the centerline and 50 mm at the side with a differential settlement of 30 mm at 48 hours. As water infiltrates, the differential settlement keeps increasing, and the maximum differential settlement reaches 80 mm at 96 hours. Figure 6(b) shows the lateral displacements of slope surface during rainfall infiltration. Similar to the settlements, the lateral displacements are small in the initial 24 hours but increase rapidly from 24 hours to 96 hours with increasing degree of saturation. The lateral displacement of slope is the largest at the elevation of approximately 4 m. In general, the displacements become stable after 120 hours, as most of the embankment becomes saturated.

Figure 7 shows the distribution of incremental shear strain during rainfall infiltration. At 24 hours, the shear strains are generally small in the embankment slope. The shear strains at the mid-height of slope start to develop at 48 hours. With the increasing of degree of saturation, shear strains start to accumulate and increase toward the toe of slope, forming an obvious plastic shear zone. In general, the potential failure surface appears at a shallow depth of approximately 2 m from the slope surface.

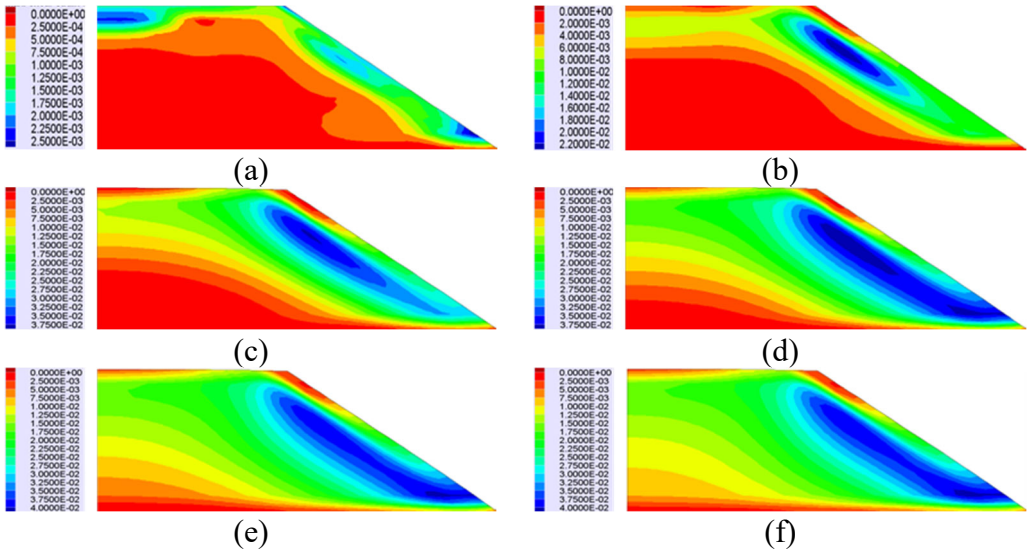

Figure 7. Distributions of shear strain: (a) T = 24h; (b) T = 48h; (c) T = 72h; (d) T = 96h; (e) T = 120h; (f) T = 144h.

CONCLUSIONS

A hydro-mechanical coupled constitutive model for unsaturated soil is proposed, which accounts for the effect of degree of saturation on the stress-strain behavior and the effect of void ratio on the water retention behavior. The proposed model is implemented in the finite difference program FLAC and calibrated using data from triaxial tests. The constitutive model for unsaturated soil implemented in FLAC used to simulate the behavior of an unsaturated embankment subjected to rainfall infiltration. As water infiltrates into the embankment, the differential settlement on the embankment top surface between the centerline and edge of the embankment increases, and the lateral displacements of slope surface also increases significantly. A potential failure surface appears at a shallow depth of approximately 2 m from the slope surface after the soil reaches full saturation. Further investigations can be conducted to explore the applicability of implemented hydro-mechanical coupled model for engineering problems involving unsaturated soils.

REFERENCES

Alonso, E. E., Gens, A., and Josa, A. (1990). "A constitutive model for partially saturated soils." *Geotechnique*, 40(3), 405-430.

Gallipoli, D., Gens, A., Sharma, R., and Vaunat, J. (2003). "An elastoplastic model for unsaturated soil incorporating the effects of suction and degree of saturation on mechanical behaviour." *Geotechnique*, 53(1), 123–135.

Le, T. M. H., Gallipoli, D., Sanchez, M., and Wheeler, S. J. (2013). “Rainfall-induced differential settlements of foundations on heterogeneous unsaturated soils.” *Geotechnique*, 63(15), 1346–1355.

Nuth, M., and Laloui, L. (2008). “Advances in modelling hysteretic water retention curve in deformable soils.” *Computers and Geotechnics*, 35(6), 835–844.

Olivella, S., Gens, A., Carrera, J., and Alonso, E. E. (1996). “Numerical formulation for a simulator (CODE_BRIGHT) for the coupled analysis of saline media.” *Engineering Computations*, 13(7), 87-112.

Rutqvist, J., Ijiri, Y., and Yamamoto, H. (2011). “Implementation of the Barcelona Basic Model into TOUGH-FLAC for simulations of the geomechanical behavior of unsaturated soils.” *Computers and Geosciences*, 37(6), 751-762.

Sun, D. A., Sheng, D. C., and Sloan, S. W. (2007). “Elastoplastic modelling of hydraulic and stress-strain behaviour of unsaturated soils.” *Mechanics of Materials*, 39(3), 212-221.

Tatsuoka F, and Gomes Correia A. (2018). “Importance of controlling the degree of saturation in soil compaction linked to soil structure design.” *Transportation Geotechnics*, 17, 3–23.

van Genuchten, M. T. (1980). “A closed-form equation for predicting the hydraulic conductivity of unsaturated soil.” *Soil Science Society of America Journal*, 44, 892–898.

Wheeler, S. J., and Sivakumar, V. (1995). “An elasto-plastic critical state framework for unsaturated soil.” *Geotechnique*, 45(1), 35–53.

Wheeler, S. J., Sharma, R. S., and Buisson, M. S. R. (2003). “Coupling of hydraulic hysteresis and stress–strain behaviour in unsaturated soils.” *Geotechnique*, 53(1), 41–54.

Xiong, Y. L., Ye, G. L., Xie, Y., Ye, B., Zhang, S., and Zhang, F., (2019). “A unified constitutive model for unsaturated soil under monotonic and cyclic loading.” *Acta Geotechnica*, 14(2), 313–328.

Zhou, A. N., Sheng, D., S. W. Sloan, and A. Gens. (2012). “Interpretation of unsaturated soil behaviour in the stress–Saturation space, I: Volume change and water retention behaviour.” *Computers and Geotechnics*, 43, 178–187.

Zhang, F., and Ikariya, T., (2011). “A new model for unsaturated soil using skeleton stress and degree of saturation as state variables.” *Soils and Foundations*, 51(1), 67–81.

Zhao, D., Zha, J., Wu, J., (2020). “Changes in daily and cumulative volumetric rainfall at various intensity levels due to urban surface expansion over China.” *Tellus A: Dynamic Meteorology and Oceanography*, 72, 1–21.

Zheng Y., Hatami K., and Miller, G. A. (2017). “Numerical simulation of wetting-induced settlement of embankments.” *Journal of Performance of Constructed Facilities*, 31(3).